Eur. Phys. J. D (2016) 70: 140
DOI: 10.1140/epjd/e2016-70143-4

THE EUROPEAN
PHYSICAL JOURNAL D

Regular Article

Low energy electron induced reactions in fluorinated acetamide – probing negative ions and neutral stable counterparts[*]

Janina Kopyra[1,a], Constanze König-Lehmann[2], Eugen Illenberger[2], Jonas Warneke[3], and Petra Swiderek[3]

[1] Siedlce University, Faculty of Sciences, 3 Maja 54, 08-110 Siedlce, Poland
[2] Institut für Chemie und Biochemie - Physikalische und Theoretische Chemie, Freie Universität Berlin, Takustrasse 3, 14195 Berlin, Germany
[3] Institut für Angewandte und Physikalische Chemie, Universität Bremen, 28334 Bremen, Germany

Received 28 February 2016 / Received in final form 11 May 2016

Abstract. Electron impact to trifluoroacetamide (CF_3CONH_2, TFAA) in the energy range 0–12 eV leads to a variety of negative fragment ions which are formed via dissociative electron attachment (DEA). The underlying reactions range from single bond cleavages to remarkably complex reactions that lead to loss of the neutral units HF, H_2O and HNCO as deduced from their directly observed ionic counterparts $(M - H_2O)^-$, $(M - HF)^-$ and $(M - HNCO)^-$. Also formed are the pseudo-halogen ions CN^- and OCN^-. All these reactions proceed dominantly via a resonance located near 1 eV, i.e., electrons at subexcitation energies trigger reactions involving multiple bond cleavages. The electron induced generation of the neutral molecules HF, H_2O and HNCO in condensed TFAA films is probed by temperature controlled thermal desorption spectrometry (TDS) which can be viewed as a complementary techniques to gas-phase experiments in DEA to directly probe the neutral counterparts.

1 Introduction

In this contribution we study reactions in gas phase and condensed phase trifluoroacetamide (TFAA, see Fig. 1) induced by low energy electrons (0–12 eV). In the gas phase experiments, a molecular beam of TFAA is crossed with an energy selected electron beam and negative ions are recorded as a function of the electron energy via mass spectrometry. The resonances observed in the fragment negative ion yields carry clear signatures of dissociative electron attachment (DEA) [1]. In the condensed phase experiments, a multilayer film of TFAA is deposited on a cryogenic metal substrate and then irradiated by an electron beam at a particular energy. Reactions in the condensed material are then probed by thermal desorption spectrometry (TDS) [2–4]. The gas phase experiments are carried out under single collision conditions, i.e., the recorded fragment ion is the result of a single collision between an electron and the molecule resulting in resonant electron attachment and the subsequent unimolecular decomposition of the transient negative ion. While a neutral product observed via TDS is instead often the result of a sequence of reactions initiated by the impinging electrons [4–6], the condensed environment may also retain immediate products of the dissociative electron-molecule encounter.

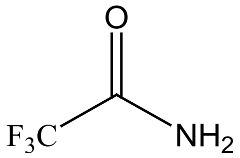

Fig. 1. Molecular structure of trifluoroacetamide.

DEA reactions have so far been studied on many compounds and, in particular, on halogenated molecules because of their well-documented electron scavenging properties [1,7]. Prototype electron scavengers are the chlorofluorocarbons (CFCs) with the peculiar properties that they are often photochemically remarkably stable, while they are very sensitive towards electrons with virtually no extra energy [8–10] thereby decomposing via DEA. Over the last 15 years or so extensive studies on biologically relevant molecules including DNA bases [11,12], sugars [13,14], and amino acids [15,16] revealed that these compounds are generally very sensitive towards low energy electrons (LEEs) [17–20], i.e., they possess low energy resonances leading to decomposition. And hence low energy electrons are considered to play a particular role in radiation damage. More precisely, the secondary electrons generated in the course of the interaction of high energy

---

[*] Contribution to the Topical Issue “Advances in Positron and Electron Scattering”, edited by Paulo Limao-Vieira, Gustavo Garcia, E. Krishnakumar, James Sullivan, Hajime Tanuma and Zoran Petrovic.

[a] e-mail: `kopyra@uph.edu.pl`

radiation with biological tissues are believed to induce reactions on a short time scale (fs-ps), which are responsible for the decisive steps ultimately leading to radiation damage [17,21].

Electron induced reactions on acetamide and some amide derivatives have previously been reported by the Berlin laboratory [22]. A prominent resonance located at 2.0 eV was observed leading to the excision of the pseudohalogen ion CN^-, which is formed via a remarkably complex unimolecular reaction.

As will be shown in the present contribution, low energy electrons trigger surprisingly complex unimolecular reactions in TFAA associated with multiple bond cleavages and the formation of stable neutral molecules like HF or H_2O, which in turn are probed by TDS. Also, we will briefly reflect on the implications of the present result with regards to control over condensed-phase electron-induced chemistry.

2 Experimental procedure

2.1 Gas phase experiment

The gas phase experiments were performed utilizing an electron/molecular crossed beams apparatus. It consists of an oven, a trochoidal electron monochromator (TEM) and a quadrupole mass spectrometer (QMS). An incident electron beam of well-defined energy (FWHM ≈ 140 meV, electron current ≈ 10 nA) generated from a TEM intersects with an effusive molecular beam. The molecular beam emanates from a capillary, which connects the vessel containing the sample of the investigated compound with the collision chamber. The sample of trifluoroacetamide (CF_3CONH_2) is solid under normal conditions. Hence in order to obtain sufficiently high vapour pressure at the collision chamber, the entire system was heated up to around 333 K. The pressure of the molecules in the gas phase measured by an ionisation gauge mounted at one of the flanges was in the range of 10^{-6} mbar.

Negative ions formed in the reaction zone are extracted from the reaction volume by a weak electric field (<1 V/cm) towards a quadrupole mass analyser and detected by a single pulse counting technique. The intensity of the respective anions is recorded as a function of the incident electron energy. The electron energy scale was calibrated using SF_6 which forms SF_6^- near 0 eV. The sample of trifluoroacetamide was obtained from Sigma Aldrich with a stated purity of 97% and used as delivered.

2.2 Condensed phase experiment

Electron-induced reactions in condensed multilayer molecular films of TFAA were investigated by post-irradiation thermal desorption spectrometry (TDS) [23]. The experiments are performed in an ultra-high vacuum chamber having a base pressure of 10^{-10} mbar. TFAA films were deposited at ~35 K on a polycrystalline Au foil by leaking a predefined amount of TFAA vapour via a gas handling manifold onto the Au substrate. It should be noted that the amount of TFAA deposited on the substrate could not be precisely controlled as the molecule was sticking to the surfaces of the inlet system. This means that after closing the inlet valve some poorly defined amount of TFAA desorbed into the vacuum chamber and condensed on the substrate. However, comparing with previous thickness calibrations for other compounds [23,24] we can deduce that the layer thickness was well in the multilayer regime.

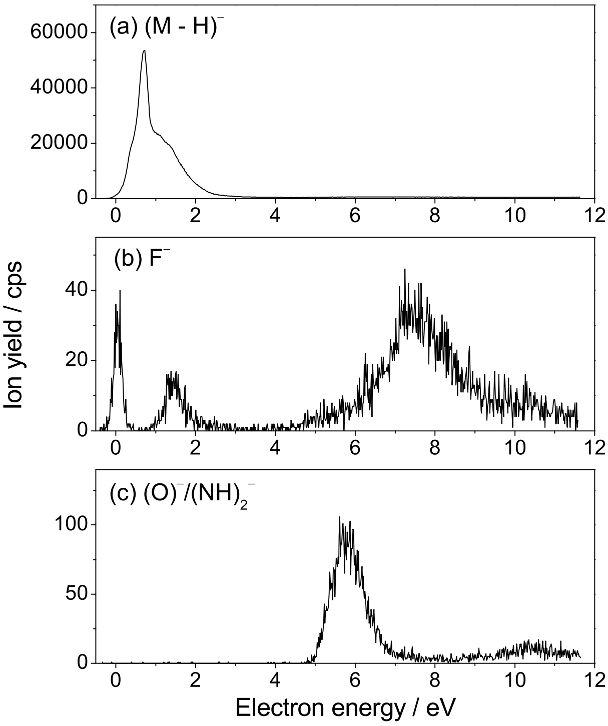

Fig. 2. Yield curves for the fragment ions $(M-H)^-$, F^- and O^-/NH_2^- that are generated from a simple bond cleavages.

The condensed films are exposed to an electron beam from a commercial flood gun (SPECS FG15/40) having an energy resolution of 0.5–1 eV. Desorbing neutral molecules are analysed by means of a quadrupole mass spectrometer (QMS) residual gas analyser (Stanford Research Systems RGA 200). The QMS is equipped with an electron impact ion source operating at an electron energy of 70 eV. Desorption was monitored after irradiation upon heating the Au foil with a rate of 1 K/s by resistive heating with Ta ribbons spot welded to the gold substrate. Typically, four different masses can be monitored simultaneously during desorption.

3 Results and discussion

3.1 Gas phase DEA reactions

The ion yield curves of the prominent negative fragment ions are presented in Figures 2–5. All ion yields show pronounced resonance profiles, indicating that they result from dissociative electron attachment (DEA). DEA

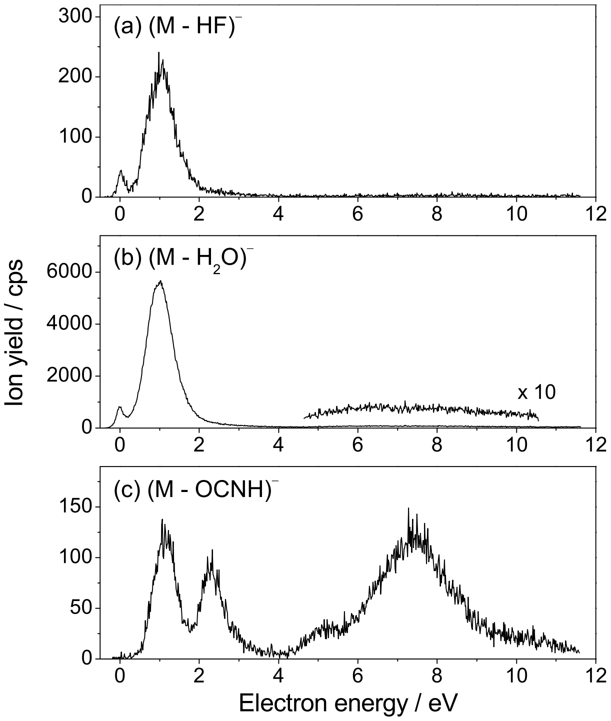

Fig. 3. Yield curves for the fragment ions $(M - HF)^-$, $(M - H_2O)^-$ and $(M - HNCO)^-$, which are associated with the loss of neutral stable molecules HF, H_2O and HNCO, respectively.

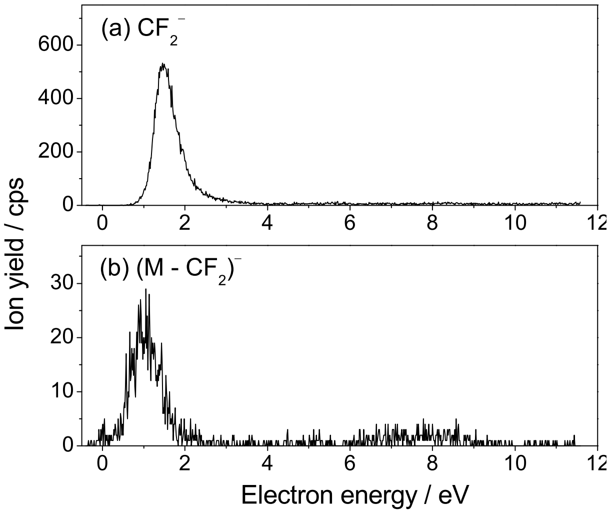

Fig. 4. Yield curves for the complementary ions CF_2^- and $(M - CF_2)^-$.

is a two-step process that creates a transient parent anion $M^{\#-}$ (where M is a target molecule), which subsequently decomposes into stable negative fragment ions and one or more neutral fragments. Concerning the electronic structure of the transient anion (resonance) one distinguishes between shape resonances and core excited resonances [1]. We can assume that the low energy features (<3 eV) can be characterised as shape resonances, where the extra electron temporarily occupies one of the normally empty molecular orbitals (MOs). The broader and overlapping features observed at 5 eV, 8.5 eV and 10.5 eV visible on the fragments F^-, $(M - H_2O)^-$, and $(M - HNCO)^-$ can be characterised as core excited resonances with possible contributions of higher lying shape resonances. A core excited resonance is associated with electronic excitation, i.e., the incoming electron causes electronic excitation with the slowed down electron temporarily trapped in the field of the electronically excited molecule. Electronic structure calculations indicated that in the structurally-related acetamide (CH_3CONH_2) the low energy extra electron resides in an MO, which is appreciably delocalised having $\pi^*_{C=O}$ character [22]. The same is presumably also the case for TFAA.

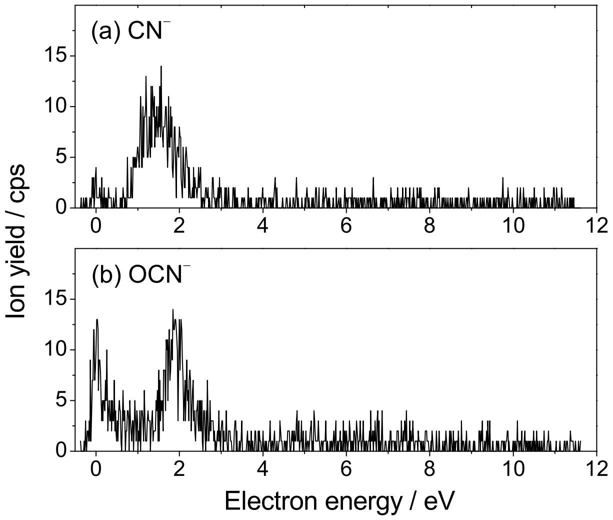

Fig. 5. Yield curves of the pseudohalogen ions CN^- and OCN^-.

Some of the ion fragments arise from the cleavage of a single bond like $(M - H)^-$, F^-, O^-/NH_2^- (Fig. 2) but also quite complex reactions occur which proceed via considerable rearrangement in the transitory anion thereby forming new molecules as seen in Figure 3.

3.1.1 Formation of $(M - H)^-$, $(M - F)^-$, and $(M - O)^-/(M - NH_2)^-$

We shall now consider the reaction pathways in more detail starting with the simple bond cleavages. Figure 2 presents the fragment anions arising from the cleavage of a single bond. By far the most prominent ion is the closed shell anion $(M - H)^-$ formed by the loss of a neutral hydrogen atom according to the DEA reaction

$$e^- + M \rightarrow M^{\#-} \rightarrow (M\text{-}H)^- + H \qquad (1)$$

with $M^{\#-}$ being the transient anion formed upon resonant free electron attachment and $(M - H)^-$ the closed shell anion formed by neutral hydrogen loss. Process (1) is ubiquitous in most organic and biological molecules [18,25]. Due to the formation of the reactive H atom radical process (1) is particularly relevant for the question of radiation damage. (M – H) radicals possess appreciable electron affinities (in the range 3–4 eV) [26] so that the corresponding

Table 1. Standard heats of formation (ΔH_f°) and electron affinities for some compounds relevant in the present reactions. If not stated otherwise taken from reference [26].

Compound	ΔH_f° (kJ mol^{-1})
CF_3CONH_2 (trifluoroacetamide)	$\approx -900^a$
CF_3CN (triflouroacetonitrile)	-495.39
HNCO (isocyanic acid)	-101.67
CHF_3	-697.05
HF	-273.3 ± 0.70
CF_3	-470.28
CF_2	-182.00
CFO	-171.54
CN	435.14
NCO	155 ± 15^b
H_2O	-241.826 ± 0.040
Compound	Electron affinity (eV)
CN	3.8620 ± 0.005
NCO	3.6090 ± 0.005
CF_2	0.180 ± 0.020
F	3.401191 ± 0.000026
O	1.439157 ± 0.000004
NH_2	0.7710 ± 0.0050

[a] Estimated from the heat of formation for acetamide (-238 kJ mol^{-1}) and assuming that for CF_3CONH_2 the same analogy holds as between the heats of formation for CH_3CH_3 (-84 kJ mol^{-1}) and CF_3CH_3 (-749 kJ mol^{-1}). [b] Reference [32].

DEA reaction is energetically accessible already at subexcitation energies, i.e., at energies below the level of electronic excitation and already close to 0 eV. In the present system the H loss obviously occurs at the N-H site and the involved bond dissociation energy is in the range of 4 eV [27].

The signal of the F^- anion is comparatively weak, and apart from the low energy region it is also observed from a broad and structured feature in the energy range extending from 5 to 11 eV. The C-F bond dissociation energy is in the range 4.5 to 5.0 eV [26,27] and thus larger than the electron affinity of F (3.4 eV, see Tab. 1) indicating that the associated DEA reaction is endothermic by more than 1 eV. We hence interpret the peak at around 1.5 eV as arising from an occupation of a $\sigma*$ state with antibonding (C-F) character whilst sharp peak right at threshold as arising from vibrationally excited target molecules (hot band transitions). Due to the peculiarities of DEA (reciprocal energy dependence of the cross section, autodetachment [25]), hot band transitions can be quite intense in spite of a low Boltzmann population. This is particularly the case when autodetachment strongly competes with DEA in the decay of the transitory ion [28,29]. The general trend in electron attachment is that the cross section increases towards lower electron energies (reciprocal energy dependence) [1]. The observation that (a) the overall intensity of F^- is comparatively low and (b) it is relatively higher within the feature peaking near 7.5 eV thus strongly suggests a significant contribution of autodetachment within the low energy region (<2 eV).

The signal of the ion of 16 amu can be attributed to either O^- or NH_2^- which both arise from a simple (double or single) bond cleavage. The C-NH_2 bond dissociation energy is in the range of 3.7 eV and C=O is in the range of 7.6 eV (in ketones) [30,31], while both the electron affinities of O (1.44 eV) and NH_2 (0.77 eV) are well established (Tab. 1) leading to thermodynamic thresholds of about 2.9 eV and 6.2 eV for NH_2^- and O^- formation, respectively. From that we conclude that the formation of O^- from the resonance peaking at 5.8 eV can be excluded, at least in the energy range below 6.2 eV.

3.1.2 Formation of $(M - HF)^-$, $(M - H_2O)^-$, and $(M - HNCO)^-$

The fragment ions shown in Figures 3–5 all arise from considerably more complex unimolecular processes. The loss of a neutral HF unit (Fig. 3a) is associated with two bond cleavages, hydrogen transfer and the formation of the HF molecule. This complex process is restricted to the energy range below 2 eV. By taking the available thermochemical data, D (C-F) $\approx$ 5 eV, D (N-H) $\approx$ 4 eV and D(H-F) = 6.1 eV [26,27] one arrives at a thermodynamic threshold of nearly 3 eV for HF loss in the neutral system, while the fragment ion $(M - HF)^-$, is already observed from the prominent resonance peaking at 1.2 eV. From that one can conclude the electron affinity of the neutral fragment (M − HF) should be larger than about 2 eV.

The loss of a water unit (Fig. 3b) also represents a remarkably complex reaction. It is observed within a prominent resonance peaking at 1.0 eV, similar to HF loss. A further weaker signal is observed in the energy range between about 5 eV and 11 eV. A possible low energy reaction is

$$e^- + CF_3CONH_2 \rightarrow CF_3CN^- + H_2O \qquad (2)$$

which implies that in the course of H_2O loss substantial electronic rearrangement in the anion takes place leading to the trifluoroacetonitrile radical anion. By taking the thermodynamic values from Table 1, we arrive at a thermodynamic threshold for reaction (2) of $\Delta H_o(2)$ = 1.7 eV − $EA(CF_3CN)$. The (adiabatic) electron affinity of CF_3CN is not known, but it is a reasonably effective electron scavenger [33]. Assuming the narrow peak right at threshold is due to a hot band transition (*vide supra*) the experimental appearance energy of the $(M - H_2O)$ ion is located at ≈0.4 eV, which implies that the electron affinity of CF_3CN must be larger than 1.3 eV. It is clear that within the feature in the energy range above 5 eV the neutral water unit may not be formed but instead the H + OH radicals can be ejected.

Loss of the neutral unit HNCO (Fig. 3c) proceeds over the entire range up to about 11 eV. A possible low energy reaction is

$$e^- + CF_3CONH_2 \rightarrow CF_3H^- + HNCO \qquad (3)$$

creating the trifluoromethane radical anion. For the neutral unit the stable forms HNCO (HN=C=O, isocyanic acid), CHNO and HCNO (fulminic acid) are known but only for isocyanic acid thermochemical data are available (Tab. 1). The reaction requires cleavage of the C-C bond, hydrogen transfer and electronic rearrangement in the neutral. With the thermochemical values from Table 1 one obtains a reaction enthalpy of $\Delta H_o(3) = 1.0$ eV $- EA(CF_3H)$. The electron affinity of trifluoromethane is not known, but with the experimental appearance energy for the ion (≈0.5 eV) we can give a lower limit of $EA(CF_3H) \geqslant 0.5$ eV. It is interesting to note that the ion $(M - HNCO)^-$ is observed up to energies of more than 10 eV. In the picture of a statistical treatment of the unimolecular decomposition in the larger fragment $(M - HNCO)^-$ nearly 70% of the available excess energy should be dissipated over the vibrational degrees of freedom [1]. It is hence surprising that the ion $(M - HNCO)^-$ is stable on a mass spectrometrical time scale in spite of a weakly bound excess electron. Qualitatively the same is true for the $(M - H_2O)^-$ fragment, which, however, appears at relatively low intensity in the 5–10 eV range.

3.1.3 Formation of the complementary ions CF_2^- and $(M - CF_2)^-$

The two complementary ions (Fig. 4) are formed by the cleavage of a C-C and a C-F bond and transfer of an F atom thereby creating $FCONH_2$ (fluorinated formamide) and CF_2 with the excess electron finally localised on either of the two fragments. While there is no data available on a compound of the form $FCONH_2$, the difluoromethylene CF_2 and its anion CF_2^- are well known compounds, the latter being an often observed fragment ion in DEA [1]. Both ions appear from the low energy resonance with the $(M - CF_2)^-$ ion yield clearly shifted to lower energy, which may indicate that the electron affinity of $(M - CF_2)$ exceeds that of CF_2.

3.1.4 Formation of the pseudohalogen ions CN^- and OCN^-

Formation of the CN^- ion (Fig. 5a) represents an excision of the central unit from the molecule, which must be accompanied by significant rearrangement of the neutral counterpart thereby forming stable molecules. In analogy to the low energy reactions discussed in acetamide [22] we propose that the following energetically favourable DEA reactions are possible

$$e^- + CF_3CONH_2 \rightarrow CN^- + H_2O + CF_3 \tag{4a}$$

$$\rightarrow CN^- + OH + CHF_3. \tag{4b}$$

Reaction (4a) is an excision of CN^- by cleaving the C-C, the C-O and the two N-H bonds and rearrangement to H_2O. The net effect is a decrease of the number of bonds from 8 in the initial molecule to 6 in the three products. In reaction (4b) the underlying mechanism is even more complex, so (4a) may be the likely reaction. Accordingly, formation of OCN^- may proceed along the following reactions

$$e^- + CF_3CONH_2 \rightarrow OCN^- + H_2 + CF_3 \tag{5a}$$

$$\rightarrow OCN^- + H + CHF_3. \tag{5b}$$

The calculated reaction enthalpies based on the data from Table 1 are 2.6 eV for both reactions (4a) and (4b) and 2.5 eV for both reactions (5a) and (5b), which is considerably above the experimentally observed appearance energy. The reason for this discrepancy may originate from the uncertainty in the estimated number for the heat of formation of the target molecule.

3.2 Probing the neutral counterparts to DEA in the condensed phase via TDS

From the gas phase results considered above, prominent DEA reactions leading to the loss of the neutral units H_2O, HF, and HNCO could be identified, as deduced from the observation of the corresponding ionic counterparts $(M - H_2O)^-$, $(M - HF)^-$ and $(M - HNCO)^-$. In order to directly observe these neutral reaction products, we have performed irradiation experiments on multilayer TFAA films at different electron energies and probed the irradiated sample by TDS.

As an example, Figure 6 shows TDS data recorded at 44 amu, 20 amu, 18 amu and 43 amu from fresh TFAA films (before irradiation) and after irradiation at an electron energy of 1.5 eV. 44 amu is the dominant signal in the mass spectrum of TFAA ($OCNH_2^+$) [26] while 20 amu, 18 amu, and 43 amu are the masses of the parent cations formed in the mass spectrum of HF, H_2O, and HNCO and should thus reveal the formation of these neutral fragmentation products. The desorption signal peaking near 200 K can be attributed to the desorption of neutral TFAA molecules and fragmentation under 70 eV electron impact in the ion source of the mass spectrometer leading to fragment ions $OCNH_2^+$, HF^+, H_2O^+, and $HNCO^+$ which are all present in the mass spectrum of gas phase TFAA acquired during leaking of TFAA vapour into the chamber (not shown here).

After irradiation, desorption peaks near 150 K in the TDS data recorded at 18 amu and 20 amu increase significantly. Furthermore, a small signal below 150 K becomes apparent for 43 amu. The new desorption peak at 150 K in the 20 amu data can be attributed to the electron induced formation of neutral HF while the small peak observed below 150 K for 43 amu points to the formation of HNCO molecules. A minor desorption signal of HF present already prior to irradiation is traced back to readsorption from the residual gas in the chamber. The same applies to the TDS signal near 150 K at 18 amu which is attributed to H_2O. Obviously, a certain amount of H_2O is condensed from the residual gas during the deposition procedure. This was confirmed by observing that the 150 K peak from the non-irradiated sample increases constantly with time between deposition of the TFAA layers and the TDS experiment. We note also that some of the small neutral molecules formed upon DEA to TFAA may not desorb

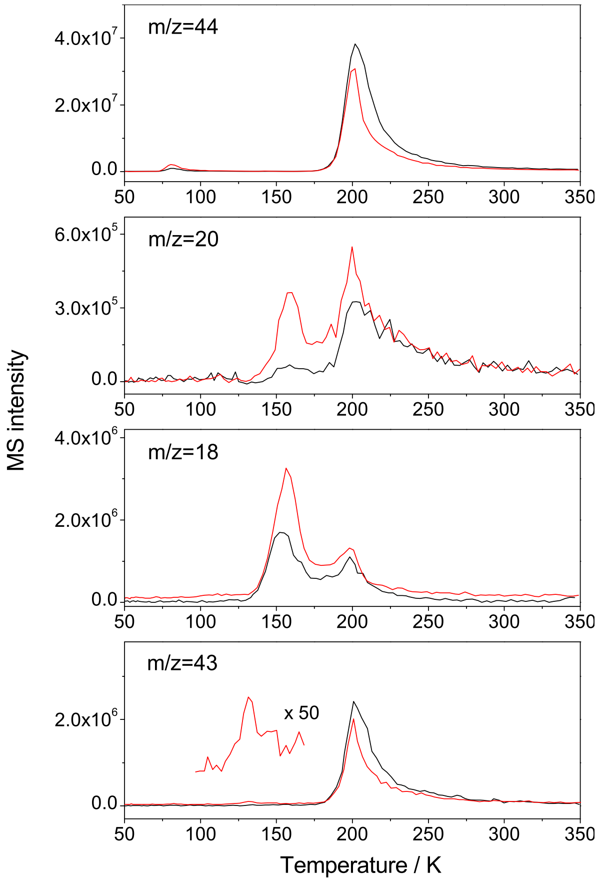

Fig. 6. Thermal desorption spectra obtained at 44 amu ($OCNH_2$), 20 amu (HF), 18 amu (H_2O) and 43 amu (HNCO) from multilayer films of CF_3CONH_2 before (black) and after (red) electron exposure of 1000 μC cm^{-2} at an incident electron energy of 1.5 eV.

freely but remain embedded in the matrix of the parent compound until the latter desorbs [34]. This accounts for some of the intensity of the 200 K desorption signals in the 18 amu and 20 amu TDS curves.

The intensity of the desorption signal at 150 K ascribed to HF decreases with the energy of the irradiating electrons as shown in Figure 7. The signal hence shows the typical reciprocal energy dependence of an electron attachment reaction [1]. Unfortunately, the energy of the irradiating electrons could not be pushed below 1.5 eV to demonstrate the resonant behaviour of the corresponding reactions. However, comparison of the gas phase width of this resonance with the range of energies in which HF formation is observed in Figure 7 points to a considerable broadening of the resonance in the condensed phase to which some charge accumulation during irradiation and consequent deceleration of the impinging electrons may also contribute.

4 Conclusions

Our results demonstrate that electron impact to gas phase TFAA leads to formation of a variety of negative ion fragments including the ions $(M - H_2O)^-$, $(M - HF)^-$ and $(M - HNCO)^-$ which are formed via DEA from a prominent resonance located near 1 eV. Because neutral fragments cannot *directly* be observed in DEA using crossed beam technique, the loss of the neutral units HF, H_2O and HNCO from the transient parent ion has been postulated from energetic considerations. These neutral counterparts, on the other hand, can *directly* be observed in thermal desorption spectrometry (TDS) following irradiation of a multilayer film at different electron energies. TDS can hence serve as a tool to directly probe the neutral counterparts in DEA.

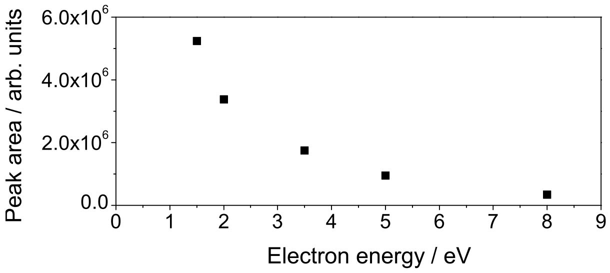

Fig. 7. Dependence of HF yields on electron energy as represented by the integrated TDS peak areas between 140 K and 175 K at $m/z = 20$ obtained from multilayer films of CF_3CONH_2 after electron exposure of 200 μC cm^{-2}.

Here, it is also interesting to observe that transition to the condensed phase and the consequent stabilization of the transient parent anion do not simply shift the HF forming resonance to lower electron energy but also broaden it noticeably. In consequence, the resonance remains accessible at electron energies that can be produced by simple non-monochromatized electron sources. This implies that such very low-energy resonances can in fact be exploited in the condensed phase to trigger selective reactions in electron-driven chemistry, a strategy proposed earlier using non-fluorinated formamide as an example [35] and pursued in recent work on the synthesis of ethanol from ethene and water driven by DEA [6].

This work is dedicated to our friend and distinguished colleague Prof. Michael Allan on the occasion of his 65th birthday. This work has been supported by the Polish Ministry of Science and Higher Education and the Deutsche Forschungsgemeinschaft. JK acknowledges support for a visit to Universität Bremen, Bremen (Germany) from the European Union via the COST Action CM1301 (CELINA).

References

1. E. Illenberger, J. Momigny, in *Gaseous Molecular Ions. An Introduction to Elementary Processes Induced by Ionization*, Topics in Physical Chemistry, edited by H. Baumgärtel, E.U. Franck, W. Grünbein (Steinkopff Verlag, Darmstadt, Springer-Verlag, New York, 1992), Vol. II
2. G. Ertl, J. Küppers, *Low Energy Electrons and Surface Chemistry* (VCH Verlagsgesellschaft., Weinheim, 1985)

3. C.R. Arumainayagam, H.-L. Lee, R.B. Nelson, D.R. Haines, RP. Gunawardane, Surf. Sci. Rep. **65**, 1 (2010)
4. E. Böhler, J. Warneke, P. Swiderek, Chem. Soc. Rev. **42**, 9219 (2013)
5. J. Warneke, W.F. Van Dorp, P. Rudolf, M. Stano, P. Papp, S. Matejcik, T. Borrmann, P. Swiderek, Phys. Chem. Chem. Phys. **17**, 1204 (2015)
6. J. Warneke, Z. Wang, P. Swiderek, J.H. Bredehöft, Angew. Chem. Int. Ed. **54**, 4397 (2015)
7. L.G. Christophorou, J.K. Olthoff, *Fundamental Electron Interactions with Plasma Processing Gases* (Kluwer Academic, New York, 2004)
8. W. Barszczewska, J. Kopyra, J. Wnorowska, I. Szamrej, J. Phys. Chem. A **107**, 11427 (2003)
9. T. Oster, A. Kühn, E. Illenberger, Int. J. Mass Spectrom. Ion Proc. **89**, 1 (1989)
10. R. Balog, J. Langer, S. Gohlke, M. Stano, H. Abdoul-Carime, E. Illenberger, Int. J. Mass Spectrom. **233**, 267 (2004)
11. H.A. Carime, S. Gohlke, E. Illenberger, Phys. Rev. Lett. **92**, 168103 (2004)
12. S. Ptasinska, S. Denifl, P. Scheier, E. Illenberger, T.D. Märk, Angew. Chem. Int. Ed. **44**, 6941 (2005)
13. S. Ptasinska, S. Denifl, P. Scheier, T.D. Mark, J. Chem. Phys. **120**, 8505 (2004)
14. I. Baccarelli, F.A. Gianturco, A. Grandi, N. Sanna, R.R. Lucchese, I. Bald, J. Kopyra, E. Illenberger, J. Am. Chem. Soc. **129**, 6269 (2007)
15. Y.V. Vasilév, B.J. Figard, V.G. Voinov, D.F. Barofsky, M.L. Deinzer, J. Am. Chem. Soc. **128**, 5506 (2006)
16. J. Kopyra, Chem. Phys. Lett. **533**, 87 (2012)
17. L. Sanche, Eur. Phys. J. D **35**, 367 (2005)
18. I. Baccarelli, I. Bald, F.A. Gianturco, E. Illenberger, J. Kopyra, Phys. Rep. **508**, 1 (2011)
19. J. Simons, Acc. Chem. Res. **39**, 772 (2006)
20. J. Kopyra, Phys. Chem. Chem. Phys. **14**, 8287 (2012)
21. L. Sanche, Nature **461**, 358 (2009)
22. C. König-Lehmann, J. Kopyra, I. Dabkowska, J. Kocisek, E. Illenberger, Phys. Chem. Chem. Phys. **10**, 6954 (2008)
23. I. Ipolyi, W. Michaelis, P. Swiderek, Phys. Chem. Chem. Phys. **8**, 180 (2007)
24. E. Böhler, J.H. Bredehöft, P. Swiderek, J. Phys. Chem. C **118**, 6922 (2014)
25. I. Bald, J. Langer, P. Tegeder, O. Ingólfsson, Int. J. Mass Spectrom. Ion Proc. **277**, 4 (2008)
26. The NIST Chemistry WebBook, `http://webbook.nist.gov`
27. *CRC Handbook of Chemistry and Physics*, edited by D.R. Lide, 78th edn. (CRC Press, Boca Raton, 1997)
28. I. Hahndorf, L. Lehr, E. Illenberger, J. Manz, Chem. Phys. Lett. **231**, 460 (1994)
29. I. Hahndorf, E. Illenberger, Int. J. Mass Spectrom. **167**, 87 (1997)
30. H. Christen, *Grundlagen der Organischen Chemie* (Otto Salle Verlag, Frankfurt am Main, Verlag Sauerländer, Aarau, 1985)
31. M. Orchin, F. Kaplan, R.S. Macomber, R.M. Wilson, H. Zimmer, *The Vocabulary of Organic Chemistry* (John Wiley & Sons, New York, 1980)
32. H. Okabe, J. Chem. Phys. **53**, 3507 (1970)
33. M. Heni, E. Illenberger, Int. J. Mass Spectrom. Ion Proc. **71**, 199 (1986)
34. E. Burean, I. Ipolyi, T. Hamann, P. Swiderek, Int. J. Mass Spectrom. **277**, 215 (2008)
35. T. Hamann, A. Edtbauer, F. Ferreira da Silva, S. Denifl, P. Scheier, P. Swiderek, Phys. Chem. Chem. Phys. **13**, 12305 (2011)